Optimal Signal Timing for Multi-Phase Intersections ⋆

Pedro Mercader * **Melkior Ornik** ** **Per-Olof Gutman** *
Ilya Ioslovich *

* *Technion – Israel Institute of Technology, Haifa, Israel (e-mail: pedro.m@technion.ac.il, peo@technion.ac.il, agrilya@technion.ac.il)*
** *University of Texas at Austin, Austin, TX, USA (e-mail: mornik@ices.utexas.edu)*

Abstract: We present an optimal signal timing policy for multi-phase intersections. The policy is optimal in the sense of minimizing the increase in the number of queuing vehicles, i.e. maximizing throughput, within one signal cycle. By introducing weights in the optimality criterion, our solution also accommodates the setting of prioritized traffic, in which it is more important for certain classes of traffic to wait for a shorter time. The proposed signal timing policy is simple to compute and implement. In particular, we show that the proposed strategy can be computed as a solution to a linear programming problem. Additionally, upon parametrizing the proposed policy with respect to the vehicle queue lengths, we analyze some aspects of the multi-cycle behavior of the closed-loop system generated by the policy, most notably convergence of the queue lengths over time. Finally, we illustrate the proposed control law with two numerical examples, one of which is based on real data collected from an existing complex multi-phase intersection.

Keywords: Road traffic; Traffic control; Optimal control; Linear programming; Piecewise affine systems

1. INTRODUCTION

Advances in traffic-sensing technology enable the deployment of traffic-responsive strategies which incorporate real-time information as opposed to historic data. In the setting of traffic intersections, this capability motivates the development of feedback control policies for signal timings based on the current situation, instead of traditional solutions based on fixed-time policies. A key property of feedback is its ability to yield robust behavior under changing conditions (Aström and Murray, 2008), e.g., variations in the rates of vehicle arrival to the intersection, which regularly occur due to changes in the traffic situation in a wider area.

Optimal signal control for traffic intersections has been the subject of significant recent research; see, e.g., De Schutter (2000); Chang and Lin (2000); Haddad et al. (2010, 2014); Ioslovich et al. (2011a,b). However, this effort has been mainly concentrated on intersections with two signal phases, using a deterministic model introduced in D'Ans and Gazis (1976). On the other hand, major traffic intersections generally exhibit far more complicated behavior, containing multiple phases, directions of travel, and a large number of lanes. The presence of such elements makes the analysis of major intersections significantly more complex. In addition, major intersections may be conducive to more sophisticated control objectives. For instance, one might desire that public transport or paying customers wait less at a given intersection, which leads to a differential traffic priority. Strategies implementing differential traffic priority have also been the subject of substantial research interest in recent years; see Christofa et al. (2013); Lin and Lo (2015); Gutman (2016); Zhao and Ioannou (2016); Khwais and Haddad (2017).

The main contribution of this paper is the development of an optimal signal timing strategy in a multi-phase intersection. The optimality criterion is the weighted sum of the increases of vehicle queue lengths within one cycle, where the existence of weights serves to enable differential traffic priority. While the optimality criterion only accounts for a single cycle, we present a stability condition for queue lengths obtained by a derived multi-cycle law in the case where intersection parameters (arrival rates, departure rates, priority weights) do not vary over time. Such an analysis makes it possible to investigate the asymptotic properties of the queue lengths under the proposed control law.

The remainder of this paper is organized as follows. Section 2 introduces the model of the intersection and presents a nonlinear optimization problem to calculate the optimal signal timings. In Section 3, we show that a solution to this problem can be obtained more quickly by solving a related linear program. Section 4 proposes a methodology for analysis of multi-cycle queue behavior based on the proposed control law. In addition, we perform stability analysis of the queue dynamics. Two numerical examples showcasing the optimal control law are presented in Section 5.

⋆ This research was financially supported by Israel Ministry of Transport and Road Safety under research contract no. 2022575.

2. PROBLEM STATEMENT

We consider a traffic intersection with I phases and J lane groups. We remind the reader of several standard definitions. A *phase* is an interval of time in which the vehicles in some of the traffic lanes which enter the intersection are allowed to pass through the intersection. If the vehicles in a particular lane are allowed to pass through the intersection during a phase, we say that such a lane is *served* by that phase. A *lane group* is merely a group of adjacent lanes at each intersection approach that are served by the same phases. Figure 2 and Figure 4 in Section 5 illustrate the above notions.

Phases in an intersection usually repeat in a predetermined order (Thakuriah and Geers, 2013). A *cycle* is a sequence of successive phases, where each phase is used once. We denote its length by C, measured in seconds. In this paper, we assume that the phase order is set a priori, and that C is constant over time and a priori known. However, lengths of particular phases (i.e., *green times*) can change over time — they are the control input in our setup. The green time for phase i at cycle indexed by the nonnegative integer T is denoted with $g_{i,T}$.

We use $a_{j,T}$ and $d_{j,T}$ to denote the arrival and departure rate, respectively, for the lane group j during the cycle T. The value of $a_{j,T}$ states how many vehicles enter the queue in a unit of time, and $d_{j,T}$ states how many vehicles exit the queue per unit of time when the vehicles in lane group j are allowed to pass the intersection. Both $a_{j,T}$ and $d_{j,T}$ are measured in vehicles per second. The number of waiting vehicles, i.e., *queue length* of the lane group j at the beginning of cycle T is denoted by $q_{j,T}$. The *weight* associated to the lane group j at cycle T is denoted by $w_{j,T}$. The weights will be used to encode different levels of priority to each lane group.

For the reader's reference, we now list all of the assumptions taken in this paper.

(A1) The phase order and cycle length C are a priori known.
(A2) Each lane group is served by adjacent phases: the first and the last phase in a cycle that can serve the lane group j are denoted with k_j and l_j, respectively.
(A3) The intersection is *isolated*, i.e., the operations are not affected by queues from an adjacent intersection.
(A4) For all $i = 1, \ldots, I$ and $T \geq 0$, $g_{i,T} \geq g_{i,min}$, and $g_{i,min}$ is a priori known.
(A5) The weights satisfy $w_{j,T} > 0$ for all $j = 1, \ldots, J$, $T \geq 0$.
(A6) The departure and arrival rates are constant within a single cycle, and satisfy $d_{j,T} > a_{j,T}$ for all $j = 1, \ldots, J$, $T \geq 0$.

Some of the above assumptions were already briefly discussed. Because of space limitations, we omit a longer discussion, and refer the reader to, e.g., Christofa et al. (2013); Haddad et al. (2010) for discussions of standard assumptions in intersection engineering. We note that Assumption (A2) is taken largely for easier notation.

The goal of the paper is to present a control policy that optimizes the signal timings, such that

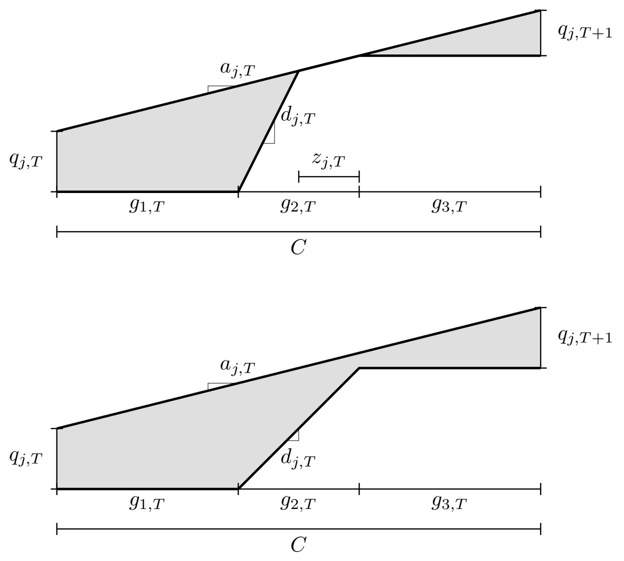

Fig. 1. Example of evolution of queue j during cycle T for $I = 3$ and $k_j = l_j = 2$. An undersaturated (oversaturated) scenario is given at the top (bottom). Upper (lower) thick line has a derivative equal to the arrival (departure) rate. The difference between the lines at any given time is equal to the queue length.

$$\sum_{j=1}^{J} w_{j,T} \left(q_{j,T+1} - q_{j,T}\right) \tag{1}$$

is minimized.

In order to obtain a simpler model, queue lengths $q_{j,T}$ are approximated by non-negative real numbers. Then, the dynamics of the queue length j are given by the following store-and-forward model:

$$\begin{aligned} q_{j,T+1} =& q_{j,T} + C a_{j,T} \\ & - \left(\sum_{i=k_j}^{l_j} g_{i,T} - z_{j,T} \right) d_{j,T} - z_{j,T} a_{j,T}, \\ & \text{for all } j = 1, \ldots, J, \end{aligned} \tag{2}$$

where $z_{j,T}$ is the *zero-queue-length period*, measured in seconds, defined as the time period for which the queue length $q_{j,T}$ is equal to zero. Given $q_{j,T}$, $g_{i,T}$, $d_{j,T}$ and $a_{j,T}$, the value of $z_{j,T}$ is determined by the following expression:

$$\begin{aligned} z_{j,T} =& \max \left(0, \sum_{i=k_j}^{l_j} g_{i,T} - \frac{q_{j,T} + \left(\sum_{i=1}^{k_j - 1} g_{i,T} \right) a_{j,T}}{d_{j,T} - a_{j,T}} \right) \\ & \text{for all } j = 1, \ldots, J. \end{aligned} \tag{3}$$

We note that model (2)–(3) covers both the situation in which there exists a time when are no cars in a particular queue (*undersaturated*), and the situation in which the queue length is always positive (*oversaturated*); see Figure 1 for an illustration.

We now formulate an optimal signal timing policy for model (2). Because of the lack of firm knowledge of arrival/departure rates in the distant future, this control policy runs cycle-by-cycle, based on queue length measurements, and the intersection parameters $a_{j,T}$, $d_{j,T}$, and $w_{j,T}$

in a given cycle. The policy is given as a solution of the following problem:

$$
\begin{aligned}
\underset{g_{i,T},\ i=1,\dots,I}{\text{minimize}} \quad & (1) \\
\text{subject to} \quad & \sum_{i=1}^{I} g_{i,T} = C \\
& g_{i,T} \geq g_{i,min}, \quad i = 1, \dots, I \\
& (2) \text{ and } (3)
\end{aligned} \tag{4}
$$

Even though (4) is nominally a nonlinear optimization problem due to the presence of $z_{j,T}$ in the cost function, we will show that its solution can be obtained from a solution of a related linear program (LP).

We note that (4) presumes knowledge of arrival and departure rates in cycle T. However, to be useful for practical purposes, an optimal control policy for cycle T would need to be calculated prior to the beginning of cycle T. In such a situation, if no prior information on $a_{j,T}$ and $d_{j,T}$ is available, the control designer may choose to use observed arrival rates $a_{j,T-1}$ and $d_{j,T-1}$ from the previous cycle as the estimates of the rates in cycle T. The same is applicable to $w_{j,T}$ in the case of changing traffic priority. Under the natural assumptions that the arrival rates change only on a time scale longer than cycle length, and departure rates remain constant throughout cycles, such a strategy produces merely a small error in the optimality of the computed policy. A more complex alternative is to use real-time traffic data collected from various sensor sources and a trained model to design predictors (Lv et al., 2015).

3. SIGNAL CONTROL VIA LINEAR PROGRAMMING

A relaxed version of the problem (4) is formulated by adding J new decision variables $\bar{z}_{j,T}$, replacing (3) by

$$
\begin{aligned}
& \bar{z}_{j,T} \geq \sum_{i=k_j}^{l_j} g_{i,T} - \frac{q_{j,T} + \left(\sum_{i=1}^{k_j-1} g_{i,T}\right) a_{j,T}}{d_{j,T} - a_{j,T}}, \\
& \bar{z}_{j,T} \geq 0, \\
& \text{for all } j = 1, \dots, J,
\end{aligned} \tag{5}
$$

and (1) by

$$
\sum_{j=1}^{J} w_{j,T} \left(C a_{j,T} - \left(\sum_{i=k_j}^{l_j} g_{i,T} \right) d_{j,T} + \bar{z}_{j,T} \left(d_{j,T} - a_{j,T}\right) \right). \tag{6}
$$

These changes guide us to the following problem:

$$
\begin{aligned}
\underset{\substack{g_{i,T},\ i=1,\dots,I \\ \bar{z}_{j,T},\ j=1,\dots,J}}{\text{minimize}} \quad & (6) \\
\text{subject to} \quad & \sum_{i=1}^{I} g_{i,T} = C \\
& g_{i,T} \geq g_{i,min}, \quad \text{for all } i = 1, \dots, I \\
& \text{and } (5).
\end{aligned} \tag{7}
$$

We now show that, in order to solve the nonlinear problem (4), it suffices to solve (7).

Proposition 1. Any optimal solution for (7) is also an optimal solution for (4).

Proof. We note that cost functions (1) and (6) coincide whenever $\bar{z}_{j,T}$ satisfy condition (3) (with $\bar{z}_{j,T}$ instead of $z_{j,T}$). Therefore, if an optimal solution

$$(g^*_{1,T}, \dots, g^*_{I,T}, \bar{z}^*_{1,T}, \dots, \bar{z}^*_{J,T})$$

of (7) satisfies (3), it can trivially be shown that $(g^*_{1,T}, \dots, g^*_{I,T})$ is an optimal solution to (4).

By Assumptions (A5) and (A6), it holds that $w_{j,T} > 0$ and $d_{j,T} - a_{j,T} > 0$. Hence, any optimal solution of (7) will exhibit the minimal possible values of $\bar{z}_{j,T}$ allowed by the constraints of (7). Thus, for each $j = 1, \dots, J$, at least one of the inequalities of (5) will be an equality. Therefore, each optimal $\bar{z}^*_{j,T}$ satisfies (3). □

4. TIME-INVARIANT SCENARIO

Having provided a cycle-by-cycle optimal control law in (7), we now focus on developing a multi-cycle law in the particular case where $d_{j,T} = d_j$, $a_{j,T} = a_j$, $w_{j,T} = w_j$ for all values of the index T. We refer to this situation as the *time-invariant scenario*. Time-invariance allows us to model the intersection as a discrete-time linear time-invariant (LTI) system whose states are the queue lengths sampled at the beginning of each cycle.

Assuming time-invariance, it is possible to write (2) as follows:

$$q_{T+1} = q_T + B u_T, \tag{8}$$

where $u_T = \left[g_{1,T} \cdots g_{I,T}\ z_{1,T} \cdots z_{J,T}\right]^\top$ and $q_T = \left[q_{1,T} \cdots q_{I,T}\right]^\top$. Matrix B is constructed by rows in the following way: for each j, $j-$th row has the entries from k_j to l_j equal to $a_j - d_j$, the rest of the first I entries are equal to a_j, and the entry $I + j$ is equal to $d_j - a_j$. All other entries are equal to zero.

4.1 Feedback Control Law

A solution to (4) depends on the queue length vector q_T, as well as the intersection parameters. In the time-invariant scenario, the parameters are assumed to be constant over the cycles. Hence, a solution to (4) (i.e., to (7)) implicity produces a single-cycle optimal feedback control law $u_T(q_T)$, with optimality given in the sense of (4). If one restricts allowed queue lengths to a polyhedron $\mathcal{Q}$, it is possible to explicitly obtain a parametric form u_T. For instance, this is possible to do by multi-parametric linear programming (mp-LP). We refer the reader to Borrelli et al. (2017) for a more detailed exposition of mp-LP.

It can be shown that the mp-LP approach produces a piecewise affine (PWA) parametric form for u_T, i.e.,

$$u_T(q_T) = A_m q_T + b_m \quad \text{if} \quad q_T \in \mathcal{R}_m \tag{9}$$

for $m = 1, \dots, M$. This form may not hold on all of $\mathcal{Q}$. However, it is defined on

$$\mathcal{S}_{\text{PWA}} = \bigcup_{m=1}^{M} \mathcal{R}_m \subseteq \mathcal{Q},$$

where matrices A_m, vectors b_m, and polyhedra $\mathcal{R}_m$ can be computed by using, e.g., Multi-Parametric Toolbox 3 (MPT) and YALMIP (Herceg et al., 2013; Löfberg, 2004).

Remark 2. We emphasize that the feedback law u_T from (9) does not guarantee optimal long-term system behavior.

Its guarantees are single-cycle: at the beginning of each signal cycle, it generates optimal behavior in that cycle. Naturally, an analogous control law with the same guarantees can be obtained for the non-time-invariant case by simply repeating the procedure in Section 3 at the beginning of every cycle. (We do note that, without time-invariance, such a law is not computable in feedback form using mp-LP, and it is not possible to easily analyze its stability.) While it would be ideal to obtain a law with firm long-term optimality guarantees, it is difficult to expect such guarantees for any real-time controller, exactly because of the lack of knowledge on traffic data in the future.

4.2 Stability Analysis

From (8) and (9), we obtain

$$q_{T+1} = f(q_T) = q_T + B\left(A_m q_T + b_m\right) \quad \text{if} \quad q_T \in \mathcal{R}_m, \tag{10}$$

for $m = 1, \ldots, M$. This relationship is well-defined for states $q_T \in \mathcal{S}_{\text{PWA}}$.

In order to describe the asymptotic behavior of the system, it is essential to discuss the presence of *equilibrium points*, i.e., points $q_{\text{eq}} \in \mathbb{R}^I$ such that $f(q_{\text{eq}}) = q_{\text{eq}}$. The set of equilibrium points $\mathcal{S}_{\text{eq}}$ of the autonomous system (10) is characterized in Proposition 3.

Proposition 3. The set $\mathcal{S}_{\text{eq}}$, that contains the equilibrium points of the autonomous system (10), is given by

$$\mathcal{S}_{\text{eq}} = \bigcup_{m=1}^{M} \left\{ q \in S_{\text{PWA}} : q \in \mathcal{R}_m \text{ and } B\left(A_m q + b_m\right) = 0 \right\}$$

The proof of Proposition 3 trivially follows from (10).

If $\mathcal{S}_{\text{eq}} \neq \emptyset$, we can assume without loss of generality that the origin is an equilibrium point for the autonomous system (10). If the origin is not an equilibrium point, it is always possible to redefine the coordinates on $\mathbb{R}^I$ in such a way that the equilibrium point of interest becomes the new origin (Vidyasagar, 2002).

Before we address the stability analysis of the autonomous system (10), let us recall standard definitions of invariance and (asymptotic) stability.

Definition 4. A set $\mathcal{O} \subseteq \mathcal{S}_{\text{PWA}}$ is a *positive invariant set* for the autonomous system (10) if $q_0 \in \mathcal{O}$ implies that $q_T \in \mathcal{O}$ for all $T > 0$.

Definition 5. A set $\mathcal{O}_\infty \subseteq \mathcal{S}_{\text{PWA}}$ is the *maximal invariant set* for the autonomous system (10) if $\mathcal{O}_\infty$ is positive invariant and contains all the positive invariant sets contained in $\mathcal{S}_{\text{PWA}}$.

Definition 6. The origin of the autonomous system (10) is *stable* if, for any $\varepsilon > 0$, there exists a $\delta(\varepsilon) > 0$, such that $\|q_0\| < \delta(\varepsilon)$ implies that $\|q_T\| < \varepsilon$ for all $T > 0$. If, in addition, $\lim_{T\to+\infty} \|q_T\| = 0$, the origin is *asymptotically stable*. Finally, let $\mathcal{X} \subseteq \mathcal{S}_{\text{PWA}}$ be a positive invariant set such that $0 \in \mathcal{X}$. The origin is *asymptotically stable on* $\mathcal{X}$ if it is asymptotically stable for any initial state $q_0 \in \mathcal{X}$.

The key to our discussion of stability of (10) is given by the following result, which we adapt from Biswas et al. (2005); Vidyasagar (2002) for our purposes.

Proposition 7. Let A_m, b_m be defined as in (9), and let B be defined as under (8). Let $\mathcal{X}$ be a positive invariant set that includes the origin. Then, the origin is asymptotically stable on $\mathcal{X}$ with dynamics (10) if there exists a (Lyapunov) function

$$V(q) : \mathcal{X} \subseteq \mathcal{S}_{\text{PWA}} \to \mathbb{R}$$

and strictly positive coefficients α, β, and γ such that

$$\begin{aligned} &\alpha\|q\| \leq V(q) \leq \|q\| \\ &V\left(q + B\left(A_m q + b_m\right)\right) - V(q) \leq -\gamma\|q\| \end{aligned}$$

for all $q \in \mathcal{R}_m$ for $m = 1, \ldots, M$.

We note that we previously made a coordinate transformation from a, potentially non-zero, equilibrium point to the origin. Thus, Proposition 7 provides a characterization of the set of initial queue lengths that will evolve towards that equilibrium under the time-invariant conditions. From a practical point of view, Proposition 7 makes it possible to determine whether the queue lengths generated by a multi-cycle law (9) will "recover" after a perturbation (e.g., a short interval of dense traffic) that moves them away from the equilibrium.

5. NUMERICAL EXAMPLES

5.1 Intersection of Two One-Way Roads

An intersection of two one-way roads ($I = J = 2$) is considered. See Figure 2 for an illustration.

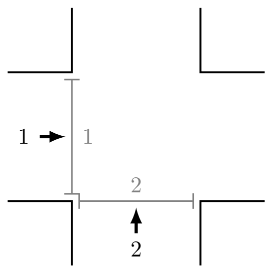

Fig. 2. Configuration of a simple intersection with two one-way phases considered in Section 5.1. Lanes group are indicated in black integer numbers from 1 to 2 and phases in gray integer numbers from 1 to 2.

We first study the time-invariant scenario characterized by the following parameters: $d_1 = 0.55$ veh/s, $d_2 = 0.60$ veh/s, $a_1 = 0.10$ veh/s, $a_2 = 0.15$ veh/s, $g_{1,min} = 5$ s, $g_{2,min} = 5$ s, $w_1 = 1$, $w_2 = 1$, $C = 30$ s.

By constraining queue lengths to belong to the set $\mathcal{Q}$ defined by $\mathcal{Q} = \left\{ [x_1 \ x_2]^\top \in \mathbb{R}^2 : 0 \leq x_1, x_2 \leq 10 \right\}$, we obtain an optimizer function $u_T(q_T)$ for $q_T \in \mathcal{Q}$ by solving the corresponding mp-LP, as discussed in Section 4.1. It can be shown that $\mathcal{S}_{\text{PWA}} = \mathcal{Q}$. Now, using Proposition 1, the control policy u_T generated by (7) is converted to optimal green times, which are given by

$$\begin{bmatrix} g_{1,T} \\ g_{2,T} \end{bmatrix} = \begin{bmatrix} 0.00 & -1.67 \\ 0.00 & 1.67 \end{bmatrix} q_T + \begin{bmatrix} 22.50 \\ 7.50 \end{bmatrix}$$

for all $q_T \in \mathcal{Q}$. By using Proposition 3, we obtain a unique equilibrium point, $q_{\text{eq}} = [0.75 \ 0.00]^\top$.

By computing the maximal positive invariant set, we obtain that $\mathcal{O}_\infty = \mathcal{S}_{\text{PWA}}$. Finally, a stability analysis shows that the autonomous system is asymptotically stable on $\mathcal{S}_{\text{PWA}}$, with the Lyapunov function computed using the Multi-Parametric Toolbox 3 (Herceg et al., 2013; Kvasnica et al., 2015). Thus, the developed feedback controller ensures that, in the long term, there will never be a queue in group lane 2 at the end of a cycle, and the queue in group lane 1 will on average be less than one vehicle at the end of each cycle. It can be easily shown that the underlying continuous-time system, where the queue lengths are also observed within traffic cycles, contains a limit cycle which passes through q_{eq}. In the interest of space, we defer a more detailed discussion to a later paper.

Figure 3 illustrates several state trajectories of the autonomous system, the polyhedral sets $\mathcal{R}_m$ used in (9), and the maximal invariant set $\mathcal{O}_\infty$.

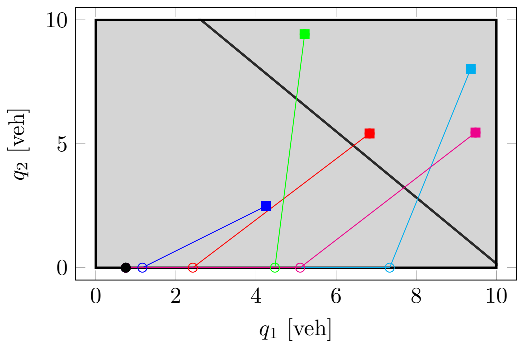

Fig. 3. State trajectories of the autonomous system of Section 5.1 for 5 random initial conditions, marked with solid squares. The last state of the trajectory (equilibrium point) is denoted with a black circle. The polygons (thick black lines) represent the sets $\mathcal{R}_m$ and the shaded area indicates the set $\mathcal{O}_\infty$.

Remark 8. With the intersection parameters given above, the system exhibits desirable properties such as uniqueness of the equilibrium point, invariance of the set where the controller is defined, and asymptotic stability. Nevertheless, we note that pathological cases may arise for different intersection parameters. For example, by changing the arrival rates to $a_1 = 0.275$ and $a_2 = 0.3$, the system exhibits infinite equilibrium points.

5.2 Multi-Phase Intersection

We now consider the optimal control of a more complex multi-phase intersection. Our work in this section is based on the major intersection of Abba Khoushy Avenue and Oscar Schindler Street in Haifa, Israel [1], whose configuration is shown in Figure 4.

The data used for intersection parameters is based on the data provided by Haifa Municipality for the morning rush hour. The parameters are as follows:

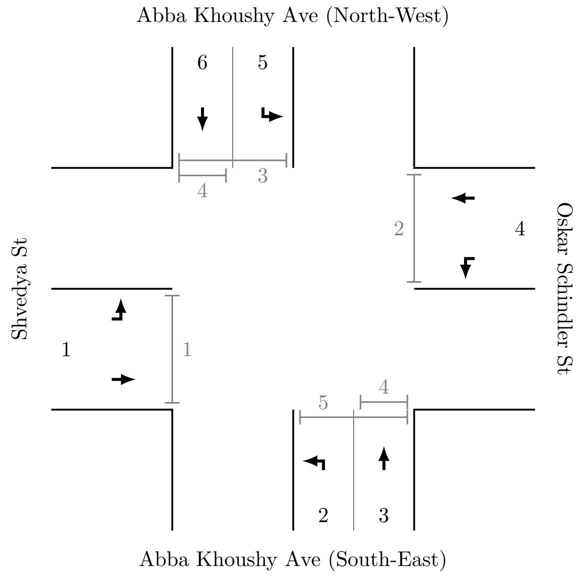

Fig. 4. Configuration of the Abba Khoushy Ave - Oscar Schindler St intersection in Haifa considered in Section 5.2. Labels and colors have an analogous role to those in Figure 2.

$$\begin{aligned}
d_j &= 1.0 \text{ veh/s} \quad \text{for all } j \in \{1,3,4,5,6\} \\
d_2 &= 0.5 \text{ veh/s} \\
a_j &= 0.1 \text{ veh/s} \quad \text{for all } j \in \{1,3,5\} \\
a_2 &= 0.02 \text{ veh/s} \\
a_4 &= 0.15 \text{ veh/s} \\
a_6 &= 0.25 \text{ veh/s}
\end{aligned}$$

The following parameters of the traffic signals are used:

$$\begin{aligned}
&g_{i,min} = 4 \text{ s} && \text{for all } i = 1,\dots,5 \\
&w_j = 1 && \text{for all } j = 1,\dots,6 \\
&C = 90 \text{ s}
\end{aligned}$$

Due to the more complicated nature of the intersection, we omit technical details present in the previous example, and concentrate on presenting the impact of the proposed control law. As in the previous section, we obtain a PWA feedback control law by solving the corresponding mp-LP. The components of q_T are constrained to belong to $\mathcal{Q} = \left\{x \in \mathbb{R}^6 : 0 \le x_i \le 15, \text{ for all } i = 1,\dots,6\right\}$. By using Proposition 3, we obtain a unique equilibrium point $q_{\text{eq}} = [4.0\ 0.0\ 0.0\ 3.975\ 0.9\ 1.0]^\top$. It is possible to prove that $\mathcal{Q}$ is the maximal positive invariant set and that the resulting autonomous system is asymptotically stable in this set. Several state trajectories (i.e., queue lengths) of the autonomous system are illustrated in Figure 5. As can be seen, the queue lengths indeed converge to q_{eq}.

Even though our algorithm does not guarantee optimal long-term behavior, we note that the proposed control law ensures that, in the long term, two lane groups are empty at the end of each cycle, two more contain at most one vehicle, and none contain more than four vehicles. On the other hand, a naive control approach which assigns equal time to each of the signal phases yields an equilibrium $[7.2\ 0.0\ 0.0\ 8.1\ 3.6\ 4.5]^\top$, which is clearly worse than q_{eq}.

[1] The satellite image from Google Maps of the area surrounding the intersection can be accessed at https://goo.gl/9G9YwW.

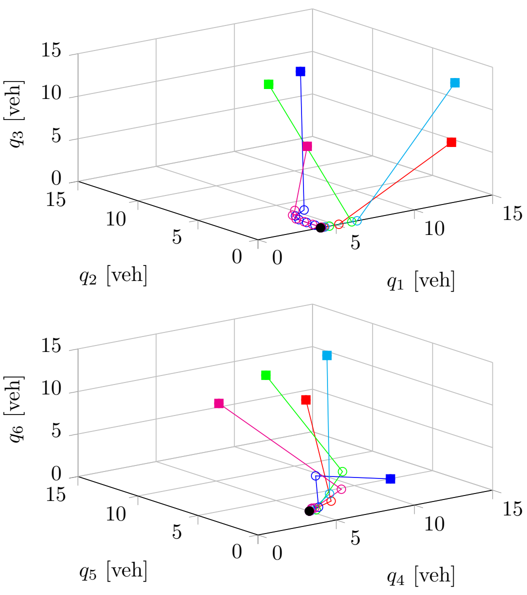

Fig. 5. State trajectories of the autonomous system of Section 5.2 for 5 random initial conditions, marked with solid squares. The last state of the trajectory (equilibrium point) is denoted with a black circle. The three first (last) components are shown at the top (bottom).

6. CONCLUSION

We propose a novel control policy for signal timing in a multi-phase intersection, and prove its optimality. The policy is simple to compute, and reduces to a linear program at each signal cycle. In a time-invariant setting, the proposed control policy can be encoded into a piecewise affine feedback form, dependent on the queue lengths at the beginning of each cycle. We present a procedure to explicitly compute such a form, and we analyze its stability.

The effect of uncertainty (or lack of knowledge) in the intersection parameters is a fundamental issue that should be addressed in future research. While developing a closed-loop structure as in this paper is the first step towards a discussion of robustness, we note that the mere use of a feedback structure does not automatically make the closed-loop system less sensitive to parameter uncertainty than an open-loop control approach.

ACKNOWLEDGEMENTS

We kindly acknowledge the Haifa Municipality for traffic data and Prof. David Mahalel, Technion, for initiating and inspiring the project.

REFERENCES

Aström, K.J. and Murray, R.M. (2008). *Feedback systems: an introduction for scientists and engineers*. Princeton University Press.

Biswas, P., Grieder, P., Löfberg, J., and Morari, M. (2005). A survey on stability analysis of discrete-time piecewise affine systems. In *16th IFAC World Congress*, 283–294.

Borrelli, F., Bemporad, A., and Morari, M. (2017). *Predictive control for linear and hybrid systems*. Cambridge University Press.

Chang, T.H. and Lin, J.T. (2000). Optimal signal timing for an oversaturated intersection. *Transportation Research Part B: Methodological*, 34(6), 471–491.

Christofa, E., Papamichail, I., and Skabardonis, A. (2013). Person-based traffic responsive signal control optimization. *IEEE Transactions on Intelligent Transportation Systems*, 14(3), 1278–1289.

D'Ans, G. and Gazis, D. (1976). Optimal control of oversaturated store-and-forward transportation networks. *Transportation Science*, 10(1), 1–19.

De Schutter, B. (2000). Optimal control of a class of linear hybrid systems with saturation. *SIAM Journal on Control and Optimization*, 39(3), 835–851.

Gutman, P.O. (2016). Dynamic pricing for toll lanes – a case study. In *14th IFAC Symposium on Control in Transportation Systems (CTS)*, 25–30.

Haddad, J., De Schutter, B., Mahalel, D., Ioslovich, I., and Gutman, P.O. (2010). Optimal steady-state control for isolated traffic intersections. *IEEE Transactions on Automatic Control*, 55(11), 2612–2617.

Haddad, J., Mahalel, D., Ioslovich, I., and Gutman, P.O. (2014). Constrained optimal steady-state control for isolated traffic intersections. *Control Theory and Technology*, 12(1), 84–94.

Herceg, M., Kvasnica, M., Jones, C.N., and Morari, M. (2013). Multi-parametric toolbox 3.0. In *2013 European Control Conference (ECC)*, 502–510.

Ioslovich, I., Gutman, P.O., Mahalel, D., and Haddad, J. (2011a). Design of optimal traffic flow control at intersection with regard for queue length constraints. *Automation and Remote Control*, 72(9), 1833.

Ioslovich, I., Haddad, J., Gutman, P.O., and Mahalel, D. (2011b). Optimal traffic control synthesis for an isolated intersection. *Control Engineering Practice*, 19(8), 900–911.

Khwais, M. and Haddad, J. (2017). Optimal pre-signal control for buses and cars at isolated signalized intersections. In *20th IFAC World Congress*, 9706 – 9711.

Kvasnica, M., Holaza, J., Takács, B., and Ingole, D. (2015). Design and verification of low-complexity explicit MPC controllers in MPT3. In *2015 European Control Conference (ECC)*, 2595–2600.

Lin, W.H. and Lo, H.K. (2015). Highway voting system: Embracing a possible paradigm shift in traffic data acquisition. *Transportation Research Part C: Emerging Technologies*, 56, 149–160.

Löfberg, J. (2004). YALMIP: A toolbox for modeling and optimization in MATLAB. In *2004 IEEE International Symposium on Computer Aided Control Systems Design*, 284–289.

Lv, Y., Duan, Y., Kang, W., Li, Z., and Wang, F.Y. (2015). Traffic flow prediction with big data: a deep learning approach. *IEEE Transactions on Intelligent Transportation Systems*, 16(2), 865–873.

Thakuriah, P.V. and Geers, D.G. (2013). *Transportation and Information: Trends in Technology and Policy*. Springer.

Vidyasagar, M. (2002). *Nonlinear systems analysis*. SIAM.

Zhao, Y. and Ioannou, P. (2016). A traffic light signal control system with truck priority. In *14th IFAC Symposium on Control in Transportation Systems (CTS)*, 377–382.